

Kinematically Optimal Hyper-Redundant Manipulator Configurations

Gregory S. Chirikjian Joel W. Burdick

School of Engineering and Applied Science
California Institute of Technology
Pasadena, CA 91125

ABSTRACT

'Hyper-redundant' robots have a very large or infinite degree of kinematic redundancy. This paper develops methods for determining the 'optimal' configurations which satisfy task constraints while minimizing a weighted measure of mechanism bending and extension. These methods are based on a continuous 'backbone curve' which captures the robot's essential macroscopic geometric features. The Calculus of Variations is used to develop differential equations, whose solution is the optimal backbone curve shape. We also consider the optimal distribution of frames along the backbone curve.

1. Introduction

'Hyper-redundant' manipulators have a very large relative degree of kinematic redundancy. In previous work [3-8], the authors have developed methods for kinematic analysis of these robots which are based on a 'backbone curve' which captures a hyper-redundant robot's macroscopic geometric features. Inverse kinematics and trajectory planning reduces to the determination of the proper time-varying backbone curve behavior. In [5,7], we considered the backbone curve shapes which arose by restricting the physically meaningful curve parameters to a modal form. This technique is used as the basis for hyper-redundant robot obstacle avoidance [4], locomotion, and grasping [6] analysis and algorithms. These papers summarize related work by other investigators.

The restriction to modal form is an arbitrary, though quite useful, restriction as it leads to very efficient inverse kinematic solutions. However, these methods are not optimal in a mathematical sense. This paper presents methods for determining backbone curve shapes which satisfy task constraints and minimize a user-defined optimality criterion. We focus on shapes which minimize a weighted measure of mechanism bending and extension. Such shapes tend to avoid actuator displacement limits. In addition, we also consider two optimality problems which arises in discretely segmented manipulator fitting procedures. An expanded version of this work can be found in [7].

In the literature several similar problems have been addressed. The optimal shape design of thin elastic rods which implement a desired robot wrist compliance was considered in [1]. The analytic techniques used in that work are similar to those used here. In [2], an efficient technique for finding the globally optimal redundant manipulator configurations was developed, though this method is most practical for a small

number of redundant degrees of freedom. [11] considers an optimal shape synthesis problem for high degree of freedom Variable Geometry Truss (VGT). The solution in [11] is an approximate one, which can be considered a subset of the modal approach presented in [4], while the method in this paper optimizes over the set of all continuous curve functions.

2. Parameterization of Backbone Curves

We assume that regardless of mechanical implementation, the important macroscopic features of a hyper-redundant robot can be captured by a backbone curve. Inverse kinematics and trajectory planning tasks are reduced to the determination of the proper time varying behavior of the backbone curve. A continuous backbone curve solution can be used to directly determine the actuator displacements of a continuous morphology robot. For discretely segmented morphologies, such as a VGT, the continuous curve solution can be used, via a 'fitting' process [5,7], to compute the actuator displacements which cause the manipulator to assume the nominal shape of the backbone curve model. We review here techniques for physically meaningful parametrization of backbone curves. A more detailed review can be found in [3].

The Cartesian location of points on a backbone curves can be intrinsically parametrized in the form:

$$\bar{x}(s, t) = \int_0^s l(\sigma, t) \bar{u}(\sigma, t) d\sigma \quad (2.1)$$

where $s \in [0, 1]$ is the parameter of the backbone curve at time t . $\bar{x}(s, t)$ is a vector from the curve base to the point s on the backbone curve. $\bar{u}(s, t)$ is the unit tangent vector to the curve at s : $l(s, t)$ length of the curve tangent and assumes the general form:

$$l(s, t) = 1 + \epsilon(s, t) > 0 \quad (2.2)$$

where $\epsilon(s, t)$ is the local extensibility of the manipulator. The extensibility provides a measure of how the parameter s differs from dimensionless arclength. $\epsilon(s, t) > 0$ indicates local extension, while $\epsilon(s, t) < 0$ implies local contraction. The parametrization of (2.1) has the following interpretation. The backbone curve is "grown" from the base by propagating the curve forward along the tangent vector, which is varying direction according to $\bar{u}(s, t)$ and varying its magnitude (or 'growth-rate') according to $l(s, t)$. In the extensible

case, the length of the backbone curve between points s_1 and s_2 is:

$$L(s_2, t) - L(s_1, t) = \int_{s_1}^{s_2} l(\sigma, t) d\sigma. \quad (2.3)$$

$L(s, t)$ is the classical arclength measure.

A *backbone reference frame* at s is a triad of right-handed orthonormal vectors, $\{\bar{e}_1(s, t), \bar{e}_2(s, t), \bar{e}_3(s, t)\}$, with frame origin coincident with point s in the curve. The orientation of the reference frames relative to a fixed frame can be expressed in matrix form as:

$$\mathbf{Q}(s, t) = (\bar{e}_1(s, t) \ \bar{e}_2(s, t) \ \bar{e}_3(s, t)) \in SO(3). \quad (2.4)$$

Note, in the remainder of this paper we drop all reference to the time dependence of curve geometry. However, all results hold in the time-varying case.

Classically, nonextensible arclength parametrized spatial curves, i.e., $L(s, t) = s$, are described using the *Frenet-Serret Apparatus*. In this system, the backbone reference frame consists of three vectors, \bar{u} , \bar{n} , and \bar{b} , where \bar{u} is as above, and:

$$\begin{aligned} \bar{n}(s) &= \frac{1}{\kappa(s)} \frac{d\bar{u}(s)}{ds} \\ \bar{b}(s) &= \bar{u} \times \bar{n}. \end{aligned} \quad (2.5)$$

$\bar{n}(s)$ and $\bar{b}(s)$ are respectively termed the normal, and binormal vectors. $\kappa(s)$ is the curvature function defined as:

$$\kappa^2 = \frac{d\bar{u}}{ds} \cdot \frac{d\bar{u}}{ds} \quad (2.6)$$

From the above definitions, the following relationships can be derived:

$$\frac{d\bar{u}}{ds} = \kappa \bar{n}; \quad \frac{d\bar{n}}{ds} = \tau \bar{b} - \kappa \bar{u}; \quad \frac{d\bar{b}}{ds} = -\tau \bar{n}. \quad (2.7)$$

where $\tau(s)$ is the *torsion* function defined as :

$$\tau = \frac{1}{\kappa^2} \bar{u} \cdot (\dot{\bar{u}} \times \ddot{\bar{u}}). \quad (2.8)$$

A $\dot{}$ represents differentiation with respect to s . $\kappa(s)$ can be physically interpreted as the bending of the curve, at s , in the plane spanned by \bar{u} and \bar{n} , while τ measures bending out of this plane.

Let $\mathbf{Q}_{FS}(s) = (\bar{u} \ \bar{n} \ \bar{b})$ denote the Frenet-Serret frames for a given curve. From (2.7), it can be seen that the rate of change of $\mathbf{Q}_{FS}(s)$ is:

$$\frac{d}{ds} \mathbf{Q}_{FS}(s) = \mathbf{Q}_{FS}(s) \begin{bmatrix} 0 & \kappa(s) & 0 \\ -\kappa(s) & 0 & \tau(s) \\ 0 & -\tau(s) & 0 \end{bmatrix} \quad (2.9)$$

Unfortunately, the Frenet-Serret apparatus is often not well suited to practical numerical computation, and alternative schemes are required. Any spherical kinematic representation can be used to parametrize $\bar{u}(s)$ in (2.1). For example, the position of points on a spatial

backbone curve can be represented by the parametric equations:

$$\bar{x}(s) = \begin{pmatrix} \int_0^s l(\sigma) \sin K(\sigma) \cos T(\sigma) d\sigma \\ \int_0^s l(\sigma) \cos K(\sigma) \cos T(\sigma) d\sigma \\ \int_0^s l(\sigma) \sin T(\sigma) d\sigma \end{pmatrix}. \quad (2.10)$$

$K(s)$ and $T(s)$ are angles which determine the direction of $\bar{u}(s)$ (fig. 1). When $T(s) = 0$ for all s , (2.10) degenerates to planar kinematics, where we denote $\theta(s) = K(s)$. By convention, $K(0) = T(0) = 0$.

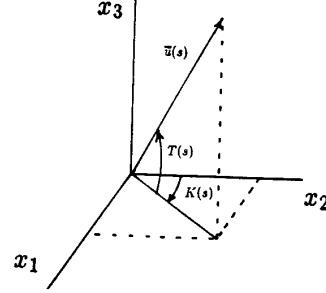


Figure 1: Physical Description of K, T

A frame can be assigned to every point on a space-curve defined by $K(s)$ and $T(s)$, as was done in the classical Frenet-Serret parameterization. This frame, referred to as the *induced reference frame* is denoted by

$$\mathbf{Q}_{IR}(s) = \begin{pmatrix} \cos K & \sin K \cos T & -\sin K \sin T \\ -\sin K & \cos K \cos T & -\cos K \sin T \\ 0 & \sin T & \cos T \end{pmatrix} \quad (2.11)$$

For consistency with previous work, the second column of \mathbf{Q}_{IR} is the backbone curve tangent vector \bar{u} . This alternate parameterization can be related to the Frenet-Serret parameters as follows:

$$\kappa^2 = \frac{1}{l^2} [(\dot{T})^2 + (\dot{K})^2 \cos^2 T] \quad (2.12a)$$

$$\tau = \frac{1}{l} [-\dot{K} \sin T + \frac{1}{\kappa^2} [(\dot{T}\dot{K} - \dot{T}\dot{K}) \cos T - (\dot{T})^2 \dot{K} \sin T]] \quad (2.12b)$$

However, for spatial backbone curves an additional function, called the roll distribution, $R(s)$, is also required to uniquely specify hyper-redundant robot configuration. The backbone reference frame, \mathbf{Q} , can be derived by rotating the induced reference frame by angle $R(s)$ about the backbone curve tangent. Thus, in this parameterization

$$\mathbf{Q}(s) = \text{ROT}[\bar{u}(s), R(s)] \mathbf{Q}_{IR}(s) \quad (2.13)$$

where $\text{ROT}[\bar{v}, \alpha]$ represents a rotation about the unit vector \bar{v} by an angle α in accordance with the right hand rule.

3. Review of Calculus of Variations

The optimal configuration problem developed in the following sections will require the minimization of integrals having the form:

$$I = \int_{s_0}^{s_1} f(s, \bar{q}(s), \bar{q}^1(s), \dots, \bar{q}^n(s)) ds. \quad (3.1)$$

$\bar{q} \in \mathbb{R}^N$ is a set of intrinsic parameters, while $f(\cdot)$ is a physically motivated function. \bar{q}^i is shorthand for $\bar{q}^i = \frac{d^i \bar{q}}{ds^i}$. (3.1) will be subject to *integral* or *isoperimetric* constraints (which arise from end-effector position constraints (2.1)) of the form:

$$\int_{s_0}^{s_1} \bar{g}(s, \bar{q}(s), \bar{q}^1(s), \dots, \bar{q}^n(s)) ds = \bar{x}_D. \quad (3.2)$$

where $s_0 = 0$, $s_1 = 1$, $\bar{g} = l\bar{u}$, and \bar{x}_D is the desired end-effector location. (3.1) may also be subject to *finite* constraints of the form:

$$\bar{h}(s, \bar{q}(s), \bar{q}^1(s), \dots, \bar{q}^n(s)) = \bar{0} \quad (3.3)$$

The Calculus of Variations [9] provides a means for finding a $\bar{q}(s)$ which yields extremal values of the (3.1) with constraints (3.2) and/or (3.3). To solve such problems, define a function (which we will call the Lagrangian):

$$\mathcal{L} = f + \bar{\mu}_c \cdot \bar{g} + \bar{\mu}_v \cdot \bar{h}. \quad (3.4)$$

where $\bar{\mu}_c$ and $\bar{\mu}_v$ are respectively constant and variable Lagrange multipliers. The $\bar{q}(s)$ which extremize (3.1) with constraints (3.2) or (3.3) is a solution to the Euler-Lagrange equations:

$$\sum_{i=0}^n (-1)^i \frac{d^i}{ds^i} \left(\frac{\partial \mathcal{L}}{\partial \bar{q}^i} \right) = 0 \quad j = 1, \dots, N. \quad (3.5)$$

With constraints (3.2) or (3.3) and boundary conditions $\bar{q}^i(s_0) = \bar{q}_0^i$ and $\bar{q}^i(s_1) = \bar{q}_1^i$ for $i \in [0, 1, \dots, n]$, (3.5) can be solved to find the extremizing functions, \bar{q} , and Lagrange multipliers $\bar{\mu}_c$ and $\bar{\mu}_v(s)$. Existence of solutions to (3.1) is discussed in [9], while numerical solutions can be found in [10].

4. Optimal Hyper-Redundant Manipulator Configurations

In an 'optimal' configuration, the set of backbone reference frames varies as little as possible from one value of s to another on the backbone curve. E.g., we are trying to find the shape which satisfies task constraints and minimizes local backbone curve bending and extension/contraction. This criterion is equivalent to the minimization of the integral:

$$I = \frac{1}{2} \int_0^1 \text{tr} \left(\dot{\mathbf{H}}(s) \mathbf{W}_4(s) \dot{\mathbf{H}}^T(s) \right) ds \quad (4.1)$$

where $\mathbf{H}(s)$ is the homogeneous transform consisting of rotation matrix $\mathbf{Q}(s)$, and position vector $\bar{x}(s)$. $\mathbf{W}_4(s)$

is a 4×4 symmetric positive definite weighting matrix with inhomogeneous units. We first consider the case of least bending for nonextensible manipulators.

4.1 Configurations of Least Bending

In this case, we seek to minimize the integral of the weighted norm of $\dot{\mathbf{Q}}(s)$ over the backbone curve length:

$$I = \frac{1}{2} \int_0^1 \text{tr} \left(\dot{\mathbf{Q}}(s) \mathbf{W}_3(s) \dot{\mathbf{Q}}^T(s) \right) ds \quad (4.2)$$

$\mathbf{W}_3(s)$ is a 3×3 symmetric positive definite weighting matrix. We make the reasonable assumption that there is no preferred direction of bending, and thus $\mathbf{W}_3(s)$ assumes the isotropic form $\mathbf{W}_3(s) = \alpha(s) \mathbf{I}_3$.

At $s = 0$, the intrinsic frame must coincide with the base frame. At $s = 1$, the intrinsic frame must correspond with the desired end-effector orientation, \mathbf{Q}_{ee} . Thus we have the boundary conditions:

$$\mathbf{Q}(0) = \mathbf{I}; \quad \mathbf{Q}(1) = \mathbf{Q}_{ee}. \quad (4.3)$$

Thus, the minimum bending problem can be stated as the minimization of (4.2) subject to constraint (2.1) ($\bar{x}(1) = \bar{x}_{ee}$) with boundary conditions (4.3). The associated Lagrangian is:

$$\mathcal{L}(s) = \frac{1}{2} \alpha(s) \text{tr} \left(\dot{\mathbf{Q}}(s) \dot{\mathbf{Q}}^T(s) \right) + \bar{\mu}_c \cdot \bar{u}(s) \quad (4.4)$$

where $\bar{\mu}_c$ is a vector of constant undetermined Lagrange multipliers arising from the isoperimetric end-effector constraint $\bar{x}(1) = \bar{x}_{ee}$. Note that in the Frenet-Serret parametrization,

$$\frac{1}{2} \text{tr} \left(\dot{\mathbf{Q}}_{SF}(s) \dot{\mathbf{Q}}_{SF}^T(s) \right) = \kappa^2(s) + \tau^2(s). \quad (4.5)$$

4.2 Configurations of Least Bending, Roll, and Extension

Now consider the general case in which the optimality criteria includes contributions from bending, roll, and elongation. A Lagrangian based on the constrained minimization of (4.1) can be written in the form:

$$\mathcal{L}(s) = \frac{1}{2} \alpha(s) \text{tr} \left(\dot{\mathbf{Q}}(s) \dot{\mathbf{Q}}^T(s) \right) + \frac{1}{2} \beta(s) (l(s) - 1)^2 + l(s) \bar{\mu}_c \cdot \bar{u}(s), \quad (4.6)$$

$\mathbf{Q}(s)$ assumes the form in (2.13) which includes roll, and $\alpha(s)$ and $\beta(s)$ weight the relative desirability of bending and extension. In [3,7], we show for the planar case that if $\alpha = r^2$ and $\beta = 1$, (4.6) measures the homogeneous kinematic deformation of a tube of radius r .

5. A Planar Nonextensible Example

In the planar case, $\mathbf{Q}(s)$ is simply a rotation by an angle $\theta(s)$ measured clockwise from the x_2 coordinate axis. It is easy to show that:

$$\frac{1}{2} \text{tr} \left(\dot{\mathbf{Q}}(s) \dot{\mathbf{Q}}^T(s) \right) = \dot{\theta}^2(s). \quad (5.1)$$

In the nonextensible case, $\theta^2 = \kappa^2$, and thus we seek to minimize:

$$I = \frac{1}{2} \int_0^1 \alpha(s) \kappa^2(s) ds \quad (5.2)$$

The forward kinematic constraint for a nonextensible planar manipulator is:

$$x_{ee} = \int_0^1 \sin \theta(s) ds; \quad y_{ee} = \int_0^1 \cos \theta(s) ds, \quad (5.3)$$

which is a degenerate form of (2.10) with $T(s) = 0, K(s) = \theta(s)$, and $l(s) = 1$. Thus, the Euler-Lagrange equation is:

$$\alpha \ddot{\theta} + \dot{\alpha} \dot{\theta} - \mu_1 \cos \theta + \mu_2 \sin \theta = 0. \quad (5.4)$$

The solution of this equation can be computed numerically, subject to constraints (5.3), and the boundary conditions $\theta(0) = 0$ and $\theta(1) = \theta_{ee}$. Note that (5.4) is similar to the classical elastica problem [12].

Configurations which are a solution to (5.3) for the special case $\alpha(s) = 1$ are shown in Figure 2. In this, and all subsequent figures, a variable geometry truss has been superimposed, or 'fitted', to the backbone curve using the procedure in [3,5].

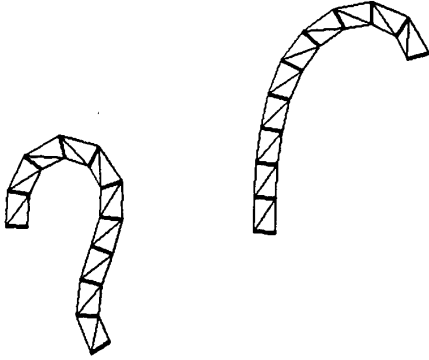


Figure 2: Optimal Planar Shapes for Uniformly Weight Curvature

In many practical cases, $\alpha(s)$ may be defined as a decreasing function, so as to minimize bending at the manipulator base. For instance, the manipulator inertial properties can be approximately incorporated by defining

$$\alpha(s) = \alpha_0 + \alpha_1 \int_s^1 \rho(\sigma) d\sigma \quad (5.5)$$

where $\rho(s)$ is the normalized mass density of the manipulator per unit curve parameter. $\int_s^1 \rho d\sigma$ is the weight of the manipulator from the distal end to point s . α_0 and α_1 weight the relative importance of uniform versus inertially weighted bending. Examples of this weighting are shown in Figure 3 for $\alpha_0 = 0.2$, $\alpha_1 = 1$, and $\rho(s) = 1$ (uniformly distributed mass).

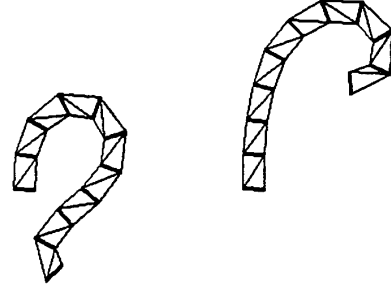


Figure 3: Optimal Planar Shapes for Curvature with Decreasing Weighting

6. A Nonextensible Spatial Example

In this example, we assume that points along the spatial backbone curve are parametrized by $K(s)$, $T(s)$, and $R(s)$. Using the parametrization in (2.13), it can be shown that:

$$\frac{1}{2} \text{tr}(\dot{Q}\dot{Q}^T) = \dot{K}^2(s) + \dot{T}^2(s) + \dot{R}^2(s) - 2\dot{K}\dot{R} \sin T(s) \quad (6.1)$$

Consequently, the constrained Euler-Lagrange equations are:

$$G(T) \begin{pmatrix} \dot{K} \\ \dot{T} \\ \dot{R} \end{pmatrix} + \bar{S}(T, \dot{K}, \dot{T}, \dot{R}) + C(T, K) \bar{\mu} = 0 \quad (6.2)$$

where:

$$G(\cdot) = \begin{pmatrix} 1 & 0 & -\sin T \\ 0 & 1 & 0 \\ -\sin T & 0 & 1 \end{pmatrix}$$

$$\bar{S}(\cdot) = (-\dot{T}\dot{R} \cos T \quad \dot{K}\dot{R} \cos T \quad -\dot{K}\dot{T} \cos T)^T$$

$$C(\cdot) = \frac{1}{2} \begin{pmatrix} -\cos K \cos T & \sin K \cos T & 0 \\ \sin K \sin T & \cos K \sin T & -\cos T \\ 0 & 0 & 0 \end{pmatrix} \quad (6.3)$$

(6.2) is solved with initial conditions $K(0) = T(0) = R(0) = 0$. The final boundary conditions can be determined by equating $Q(1)$ to the desired end-effector orientation, Q_{ee} . One of the two solutions to this problem is:

$$T(1) = \sin^{-1}(q_{ee,32})$$

$$K(1) = \text{atan2} \left(\frac{q_{ee,12}}{\cos T(1)}, \frac{q_{ee,22}}{\cos T(1)} \right) \quad (6.4)$$

$$R(1) = \text{atan2} \left(-\frac{q_{ee,31}}{\cos T(1)}, \frac{q_{ee,33}}{\cos T(1)} \right)$$

where $q_{ee,ij}$ is the i - j element of Q_{ee} . Optimal spatial configurations which arise from the solution to (6.2)

are shown in Figure 4. Here again, a variable geometry truss was 'fitted' to the optimal backbone curve for clarity. Note that $G(T)$ (which must be inverted in numerical solutions of (5.11)) will become singular when $\sin T = 1$. [3] considers 4-parameter descriptions of orientation which avoids these singularities.

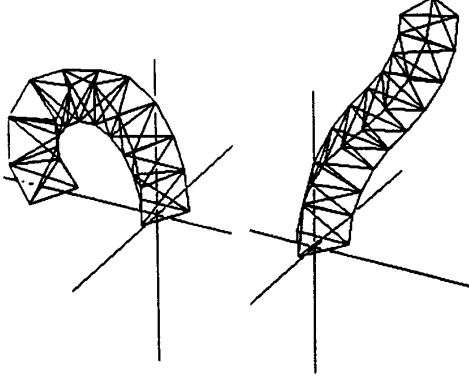


Figure 4: Optimal Spatial Configurations

7. Optimal Backbone Curve Reparameterization

Consider the reparameterization of a given planar backbone curve to minimize the variation in the backbone reference frames from one value of the curve parameter to another. This reparameterization minimizes the relative amount of local extension and bending, thereby avoiding actuator limits during the fitting process.

Let $\bar{y}^*(\phi)$ be an existing planar curve with curve parameter $\phi \in [0, \phi_0]$. We wish to find an alternative parameterization, s , such that the curve $\bar{y}(s) = \bar{y}^*(\phi(s))$ has the same shape as $\bar{y}^*(\phi)$, but that the distribution of frames on the curve vary as little as possible from one value of s to another. In other words, we wish to find a new parametrization which minimizes the planar version of (4.1) which is

$$I = \int_0^1 f(s) ds = \int_0^1 (r^2 \dot{\theta}^2 + l^2) ds \quad (7.1)$$

for isotropic and uniform weighting of bending and extension.

Reparameterization can be achieved as follows. The angle which the tangent vector \bar{y}'^* (where a ' indicates differentiation with respect to ϕ) makes with the x_2 coordinate axis is:

$$\theta^*(\phi) = \text{Atan2}(y_1', y_2'). \quad (7.2a)$$

Equate the parametrizations in ϕ and s :

$$\theta(s) = \theta^*(\phi(s)). \quad (7.2b)$$

Similarly, the local extensibility function in the new parameter s must be:

$$l^2(s) = (\bar{y}'^*(\phi(s)) \cdot \bar{y}'^*(\phi(s))) \dot{\phi}^2 \quad (7.3)$$

Thus we can write:

$$f(s) = \frac{1}{2} \left(r^2 \left(\frac{\partial \theta^*}{\partial \phi} \right)^2 \dot{\phi}^2 + (\bar{y}'^*(\phi(s)) \cdot \bar{y}'^*(\phi(s))) \dot{\phi}^2 \right) \quad (7.4)$$

which can be expressed in component form as

$$f(s) = \frac{\dot{\phi}^2}{2} \left[(y_1')^2 + (y_2')^2 + r^2 \frac{y_1'' y_2' - y_1' y_2''}{(y_1')^2 + (y_2')^2} \right] = \dot{\phi}^2 g(\phi) \quad (7.5)$$

where the superscript * has been temporarily suppressed.

The Euler-Lagrange equations are simply:

$$2\ddot{\phi}g(\phi(s)) + \dot{\phi}^2 \frac{\partial g(\phi(s))}{\partial \phi} = 0 \quad (7.6)$$

It can be shown [3,7] that the solution to (7.6) leads to the optimal reparameterization of a curve segment of length $L_0 = \int_0^{\phi_0} |d\bar{y}^* / d\phi| d\phi$:

$$s(\phi) = \frac{\int_0^\phi g^{\frac{1}{2}}(\nu) d\nu}{\int_0^{\phi_0} g^{\frac{1}{2}}(\nu) d\nu} \quad (7.7)$$

where $s() = \phi^{-1}()$.

For example, consider an arclength parametrized planar curve, $\bar{y} = \bar{y}(L)$. The optimal reparameterization is:

$$s(L) = \frac{\int_0^L (1 + r^2 \kappa^2(\nu))^{\frac{1}{2}} d\nu}{\int_0^{L_0} (1 + r^2 \kappa^2(\nu))^{\frac{1}{2}} d\nu} \quad (7.8)$$

For example, assume a nonextensible backbone curve shape which satisfies task constraints has been found using a modal approach [3,5,7]. For fitting purposes, the backbone curve can be 'optimally' reparameterized by specifying:

$$l(s) = \frac{\int_0^{L_0} (1 + r^2 \kappa^2(\nu))^{\frac{1}{2}} d\nu}{(1 + r^2 \kappa^2(L(s)))^{\frac{1}{2}}}. \quad (7.9)$$

This procedure is illustrated in Figure 5. A variable geometry truss is fitted to the backbone curve such that the spacing between truss modules is defined by (7.9). While the backbone curve is nonextensible, the variable geometry truss is extensible, and thus the truss modules can locally extend or contract. With $r = 0$, the truss modules are uniformly spaced along the backbone curve. As r increases, the spacing of the truss modules becomes increasingly nonuniform for high curvature backbone curve segments.

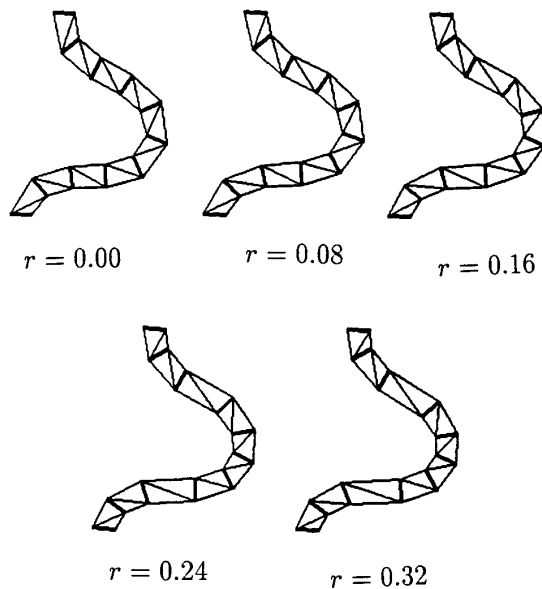


Figure 5: Optimal Reparameterization of Backbone Curves

Now let's determine the optimal roll distribution which minimizes twisting per unit length about the spatial backbone curve. This procedure is useful for determining roll distributions after a backbone curve shape has been specified to perform a particular task. Assume that $\dot{K}(s)$ and $T(s)$ have been specified. We seek to determine $R(s)$ which minimizes (4.1). The norm used in (6.1) is used here, only now we have one free variable: the roll distribution, $R(s)$.

The Euler-Lagrange equation for this problem is trivial:

$$\frac{d}{ds} (\dot{R}(s) - \dot{K}(s) \sin T(s)) = 0. \quad (7.10)$$

This equation has solution:

$$R(s) = \dot{R}(0)s + \int_0^s \dot{K}(\sigma) \sin T(\sigma) d\sigma \quad (7.11)$$

Where $\dot{R}(0)$ is selected so that the constraint on $R(1)$ is satisfied.

8. Conclusions

This paper developed methods based on the Calculus of Variations and a continuous backbone curve model for determining 'optimal' hyper-redundant manipulator configurations. The complexity of this problem was significantly reduced by using physically meaningful backbone curve parametrizations. We focused on minimizing a weighted sum of backbone curve bending, twisting, and extension. Other optimality criteria can be developed and treated in an analogous manner. We also developed means to optimally reparametrize backbone curve arclength measures and roll distributions. These problems arise when fitting discretely segmented or modular hyper-redundant mechanisms to continuous backbone curve solutions.

In previous work, the authors have developed alternative 'modal' approaches to the hyper-redundancy resolution. Both approaches are compared and contrast in [3]. In brief, the modal approach gives the user greater control over manipulator shape through the choice of intrinsic shape functions. The 'optimal' approach requires intuition in defining an appropriate cost function. The inverse kinematic solutions in both cases are cyclic because manipulator configurations are determined by a reduced set of intrinsic variables with the same dimension as the workspace.

9. References

- [1] Brockett, R.W., Stokes, A., "On the Synthesis of Compliant Mechanisms," *1991 IEEE Conference on Robotics and Automation*, pp. 2168-2173.
- [2] Burdick, J.W., Cetin, B., Barhen, J., "Efficient Global Redundant Configuration Resolution via Sub-Energy Tunneling and Terminal Repelling," *Proc. IEEE Int. Conf on Robotics and Automation*, pp. 929-944.
- [3] Chirikjian, G.S., "Theory and Applications of Hyper-Redundant Robotic Mechanisms," Ph.D thesis, Dept. of Applied Mechanics, California Institute of Technology, June, 1992.
- [4] Chirikjian, G.S., Burdick, J.W., "An Obstacle Avoidance Algorithm for Hyper-Redundant Manipulators," *Proc. IEEE Int. Conf. Robotics and Automation*, Cincinnati, OH, May 13-18, 1990.
- [5] Chirikjian, G.S., Burdick, J.W., "Parallel Formulation of the Inverse Kinematics of Modular Hyper-Redundant Manipulators," *Proc. IEEE Int. Conf. Robotics and Automation*, Sacramento, CA, April, 1991.
- [6] Chirikjian, G.S., Burdick, J.W., "Kinematics of Hyper-Redundant Locomotion with Applications to Grasping," *Proc. IEEE Int. Conf. Robotics and Automation*, Sacramento, CA, April, 1991.
- [7] Chirikjian, G.S. and Burdick, J.W., "On the Determination of Kinematically Optimal Hyper-Redundant Manipulator Configurations," *Robotics and Mechanical Systems Report no. RMS-91-02*, California Institute of Technology, September, 1991.
- [8] Chirikjian, G.S., Burdick, J.W., "Design, Implementation, and Experiments with a 30 Degree-of-Freedom Hyper-Redundant Robot," to appear in the *Proc. Int. Symp. Robotics and Manufacturing*, Albuquerque, NM, Nov., 1992.
- [9] Ewing, G.M., *Calculus of Variations With Applications*, W.W. Norton and Co. Inc., New York, 1969.
- [10] Gruver, W., Sachs, E., *Algorithmic Methods in Optimal Control*, Pitman Publishing Ltd., Melbourne.
- [11] Tavakkoli, S., Dhande, S.G., "Shape Synthesis and Optimization Using Intrinsic Geometry" *Proc. ASME Design Conference*, Chicago, IL, Sept. 16-19, 1990.
- [12] Wilson, J.F., Mahajan, U., "The Mechanics and Positioning of Highly Flexible Manipulator Limbs," *Journal of Mechanisms, Transmissions, and Automation in Design*. Vol. 111, June 1989.